6th European Conference on Computational Mechanics (ECCM 6)
7th European Conference on Computational Fluid Dynamics (ECFD 7)
1115 June 2018, Glasgow, UK

A STABILIZED PGD MIXED FORMULATION OF THE NAVIER-STOKES EQUATION, APPLICATION TO A LID-DRIVEN CAVITY

CHADY GHNATIOS[1], RAWAD HIMO[2] AND ELIE HACHEM[3]

[1] Notre Dame University - Louaize
Mechanical engineering department P.O. Box 72, Zouk Mikhael, Zouk Mosbeh, Lebanon
cghnatios@ndu.edu.lb

[2] Notre Dame University - Louaize
Thermo-fuids Research Group, P.O. Box: 72 Zouk Mikael, Zouk Mosbeh, Lebanon
rshimo@ndu.edu.lb

[3] MINES ParisTech
PSL Research University 60 Boulevard Saint-Michel, 75006 Paris, France
elie.hachem@mines-paristech.fr

Key words: Navier-Stokes, stabilization, FEM, PGD, Galerkin Least Squares

Abstract. The PGD formulation is extensively applied in different computational domains. Its recent developments target fluid behaviour in Stokes and linear Ericksen flow formulation using Penalty formulation or stable P1/P2 formulations to overcome the LBB condition. In this work, we derive a stabilized PGD formulation for the non-linear Navier-Stokes equation using Galerkin Least Squares including the convective term. The derived formulation is used to solve benchmark problems like the lid-cavity using the PGD domain decomposition. The obtained solution is stable even using same linear interpolation functions P1/P1 for the velocity and the pressure in all PGD subdomains.

1 INTRODUCTION

The demanding industrial applications constantly require faster numerical techniques, despite the enhancement in computational power. Therefore, model order reduction techniques (MOR) have been actively researched. The Proper Generalized Decomposition (also known as PGD), is one of the active MOR research domains, since it is an *a priori* model order reduction technique that requires no prior knowledge of the expected solution. Having produced very good results in various problems of physics and engineering [3, 4, 5], either in complex or hexahedral domains [7, 8], the application of the PGD in fluid mechanics remains mostly restricted to the use of the penalty approach on the stokes equations, neglecting the convective terms, rather than coupling the velocities and pressure by a mixed formulation [6]. Some studies have tried to upgrade the method by employing it to the Navier-Stokes equations and the Rayleigh Bernard non linear flows,

however several approximations were used [9, 10]. The objective of this work is to derive a stabilized PGD mixed formulation for the Navier-Stokes equation, not using any mesh conditioning, and thereby reducing the computational time significantly [2]
Numerical solution of the incompressible fluid flow is known to be complicated to achieve due to the necessity of achieving the conservation of mass on one hand, and dealing with the subgrid phenomena on the second hand. Adding to this the issue of model order reduction techniques and separated representation, special care must be taken to achieve convergence of the PGD. While the Ladyzhenskaya-Babuska-Breezi(LBB) condition (also known as the $inf - sup$ condition) has been tackled on an Eriksen flow using the (PGD) [11] the Navier-Stokes equations are still not yet solved using the PGD in a mixed formulation, using the same interpolation functions for velocity and pressure fields.
The present study hence tackles the aforementioned Navier-Stokes stabilization using the Galerkin Least Squared (GLS) method to interpolate the velocities and pressures [12], since the GLS success has well been validated in previous studies in various fields [13, 14, 15, 16]. Subsequently, we will present the governing equations with the stabilization technique, followed by a brief elaboration on the proper generalized decomposition, and finally numerical results will be shown for a benchmark problem, the lid driven cavity flow for instance.

2 NUMERICAL METHOD

2.1 Governing equations

In this work, for sake of simplicity and without any loss of generality, the flow field is governed by the two-dimensional (2D) steady-state Navier Stokes equations. The continuity and momentum equations for an incompressible Newtonian fluid in their strong forms are written as:

$$\begin{cases} \nabla \cdot \mathbf{u} = 0 \\ \rho \left(\mathbf{u} \cdot \nabla \mathbf{u} \right) = -\nabla p + \nabla \cdot \mathbb{S} \end{cases} \tag{1}$$

where $\mathbf{u}$ is the velocity vector field, p the pressure field and ρ the density. In the linear momentum equation $\mathbb{S}$ is the viscous stress tensor written by:

$$\mathbb{S} = \mu \left[\nabla \mathbf{u} + \nabla \mathbf{u}^T \right] \tag{2}$$

where μ is the dynamic viscosity of the working fluid.

Let ∇^S be the symmetrical component of the gradient tensor:

$$\nabla^S = \frac{1}{2} \left(\nabla + \nabla^T \right) \tag{3}$$

Hence the momentum equation could be re-written as follows:

$$\rho \left(\mathbf{u} \cdot \nabla \mathbf{u} \right) = -\nabla p + \nabla \cdot \left(2\mu \nabla^S \mathbf{u} \right) \tag{4}$$

The weak form is subsequently derived as such:

$$\begin{cases} \int_\Omega p^* \nabla \cdot \mathbf{u} d\Omega = 0 \\ \int_\Omega \mathbf{u}^* \rho \left(\mathbf{u} \cdot \nabla \mathbf{u} \right) d\Omega - \int_\Omega p \nabla \mathbf{u}^* d\Omega + \int_\Omega \left(\nabla^S \mathbf{u}^* \right) : \left(2\mu \nabla^S \mathbf{u} \right) d\Omega = 0 \end{cases} \tag{5}$$

where all superscripts $*$ refer to the test functions of the corresponding variable. Further simplifications on the notation could be introduced by the use of the bilinear form notation as follows:

$$\begin{cases} a\left(\mathbf{u}^*, \mathbf{u}\right) = \int_\Omega \mathbf{u}^* \rho \left(\mathbf{u} \cdot \nabla \mathbf{u} \right) d\Omega \\ b\left(p^*, \mathbf{u}\right) = -\int_\Omega p^* \nabla \mathbf{u} d\Omega \\ c\left(\mathbf{u}^*, \mathbf{u}\right) = \int_\Omega \left(\nabla^S \mathbf{u}^* \right) : \left(2\mu \nabla^S \mathbf{u} \right) d\Omega \end{cases} \tag{6}$$

Hence, the conservation of mass and momentum could be re-written by:

$$\begin{cases} b\left(p^*, \mathbf{u}\right) = 0 \\ a\left(\mathbf{u}^*, \mathbf{u}\right) + b\left(p, \mathbf{u}^*\right) + c\left(\mathbf{u}^*, \mathbf{u}\right) = 0 \end{cases} \tag{7}$$

Since the convergence of Equations (7) depends on the coercivity of the bilinear form c and the satisfaction of the $inf - sup$ condition of operator b, mesh based finite elements method with linear interpolation functions on the pressure p and velocity field $\mathbf{u}$ fail to depict the exact solution. Therefore, we adopt the Galerkin Least Squares (GLS) method to stabilize the weak formulation using linear interpolation functions for both p and $\mathbf{u}$. The GLS write the stabilized problem as proposed by [17] using:

$$\begin{cases} b\left(p^*, \mathbf{u}\right) - \sum_{e=1}^{n_{el}} \tau_3 \left(\nabla p^*, \nabla p \right)_{\Omega_e} - \sum_{e=1}^{n_{el}} \tau_4 \left(\nabla p^*, \rho \mathbf{u} \nabla \mathbf{u} \right)_{\Omega_e} = 0 \\ a\left(\mathbf{u}^*, \mathbf{u}\right) + b\left(p, \mathbf{u}^*\right) + c\left(\mathbf{u}^*, \mathbf{u}\right) + \sum_{e=1}^{n_{el}} \tau_1 \left(\rho \mathbf{u} \nabla \mathbf{u}^*, \rho \mathbf{u} \nabla \mathbf{u} \right)_{\Omega_e} \\ + \sum_{e=1}^{n_{el}} \tau_2 \left(\rho \mathbf{u} \nabla \mathbf{u}^*, \nabla p \right)_{\Omega_e} = 0 \end{cases} \tag{8}$$

The exact values of the parameters τ_i can only be determined empirically [18]. For a thorough discussion on the Galerkin Least Squares stabilization in a finite element framework, one can refer to [17, 18] and their references therein.

2.2 Linearizing the Navier-Stokes equation

To solve the weak formulation illustrated in equation (5), a linearization step of the advective term is mandatory. Therefore, the simplest choice of a fixed point iterative algorithm is used, considering the operator a defined in equation (6) as:

$$a\left(\mathbf{u}^*, \mathbf{u}\right) = \int_\Omega \mathbf{u}^* \rho \left(\mathbf{u}_c \cdot \nabla \mathbf{u} \right) d\Omega \tag{9}$$

where $\mathbf{u}_c$ is the known best estimation of $\mathbf{u}$. In practice, $\mathbf{u}_c$ is initialized as the solution of the Stokes equation, a linear problem, using the same boundary conditions as the solved

Navier-Stokes problem. Later on, an iterative fixed point algorithm is used to update $\mathbf{u}_c$ from the currently computed $\mathbf{u}$, until the convergence of $\mathbf{u}_c$.

2.3 Proper generalized decomposition (PGD)

To reduce the computational time of solving the aforementioned governing equations, stabilized using the Galerkin Least Square formulation, the model order reduction technique PGD is employed. Therefore the $2D$ domain Ω could be decomposed and solved sequentially as $1D \times 1D$ problem. The solution of the GLS stabilized equations (8) writes in a separated form $(\mathbf{u}, p)$ by:

$$\begin{pmatrix} \mathbf{u} \\ p \end{pmatrix} \approx \begin{pmatrix} \sum_{i=1}^{N} \mathbf{X}_\mathbf{i}^\mathbf{u}(x) \circ \mathbf{Y}_\mathbf{i}^\mathbf{u}(y) \\ \sum_{i=1}^{N} X_i^p(x) \cdot Y_i^p(y) \end{pmatrix} \tag{10}$$

where $\circ$ refers to the Hadamard product i.e. term by term multiplication of the $\mathbf{X}_\mathbf{i}^\mathbf{u}(x)$ and $\mathbf{Y}_\mathbf{i}^\mathbf{u}(y)$. The PGD algorithm is characterized by linear addition of the enrichment modes. Consider the computed solutions of $n-1$ modes, noted u^{n-1}, the n^{th} enrichment mode sought to find u^n could be calculated as such:

$$\begin{pmatrix} \mathbf{u} \\ p \end{pmatrix}^n = \begin{pmatrix} \sum_{i=1}^{n-1} \mathbf{X}_\mathbf{i}^\mathbf{u}(x) \circ \mathbf{Y}_\mathbf{i}^\mathbf{u}(y) + \mathbf{R}(x) \circ \mathbf{S}(y) \\ \sum_{i=1}^{n-1} X_i^p(x) \cdot Y_i^p(y) + T(x) \cdot U(y) \end{pmatrix} = \begin{pmatrix} \mathbf{u}_{n-1} + \mathbf{R}(x) \circ \mathbf{S}(y) \\ p_{n-1} + T(x) \cdot U(y) \end{pmatrix} \tag{11}$$

Following this notation the gradient of the velocity vector field $\mathbf{u} = (u_x, u_y)$ is depicted by:

$$\nabla \mathbf{u}^n = \begin{pmatrix} \frac{\partial u_x}{\partial x} & \frac{\partial u_x}{\partial y} \\ \frac{\partial u_y}{\partial x} & \frac{\partial u_y}{\partial y} \end{pmatrix}^n =$$

$$\sum_{i=1}^{n-1} \begin{pmatrix} \frac{\partial X_i^{u_x}}{\partial x} & X_i^{u_x} \\ \frac{\partial X_i^{u_y}}{\partial x} & X_i^{u_y} \end{pmatrix} \circ \begin{pmatrix} Y_i^{u_x} & \frac{\partial Y_i^{u_x}}{\partial y} \\ Y_i^{u_y} & \frac{\partial Y_i^{u_y}}{\partial y} \end{pmatrix} + \begin{pmatrix} \frac{\partial R^{u_x}}{\partial x} & R^{u_x} \\ \frac{\partial R_i^{u_y}}{\partial x} & R^{u_y} \end{pmatrix} \circ \begin{pmatrix} S^{u_x} & \frac{\partial S^{u_x}}{\partial y} \\ S^{u_y} & \frac{\partial S^{u_y}}{\partial y} \end{pmatrix} = \tag{12}$$

$$\sum_{i=1}^{n-1} \mathcal{X}_i^\mathbf{u} \circ \mathcal{Y}_i^\mathbf{u} + \mathcal{R} \circ \mathcal{S}$$

Whereas the pressure gradient is written by:

$$\nabla p^n = \begin{pmatrix} \frac{\partial p}{\partial x} \\ \\ \frac{\partial p}{\partial y} \end{pmatrix}^n \approx \sum_{i=1}^{n-1} \begin{pmatrix} \frac{\partial X_i^p}{\partial x} \\ \\ X_i^p \end{pmatrix} \cdot \begin{pmatrix} Y_i^p \\ \\ \frac{\partial Y_i^p}{\partial y} \end{pmatrix} + \begin{pmatrix} \frac{\partial T}{\partial x} \\ \\ T \end{pmatrix} \cdot \begin{pmatrix} U \\ \\ \frac{\partial U}{\partial y} \end{pmatrix} = \sum_{i=1}^{n-1} \mathcal{X}_i^p \cdot \mathcal{Y}_i^p + \mathcal{T} \cdot \mathcal{U} \tag{13}$$

The most appropriate choice of the test functions $\mathbf{u}^*$ and p^* in the separated representation framework is:

$$\begin{cases} \mathbf{u}^* = \mathbf{R}^* \circ \mathbf{S} + \mathbf{R} \circ \mathbf{S}^* \\ \\ p^* = T^* \cdot U + T \cdot U^* \end{cases} \tag{14}$$

where $\mathbf{R}^*$ and T^* are test functions that only depend on x, whereas the test functions $\mathbf{S}^*$ and U^* are similarly exclusively depending on y. Having defined the gradients in equations (12) and (13) and the test functions in equation (14), the weak form of the governing equations (7) could be solved [19]. The resulting nonlinear equation comprising four unknowns could be linearized by the use of a fixed-point iterative algorithm. First, we consider $\mathbf{S}$ and U, the y components of each of the velocity vector and pressure field as unknowns, and compute the $\mathbf{R}$ and T. Subsequently, the unknowns $\mathbf{S}$ and U could be computed. Alternations of the computation of $\mathbf{R}$ & T at a time, and $\mathbf{S}$ & U at another, are carried until convergence of each enrichment mode. The algorithm is further elaborated in subsections 2.3.1 and 2.3.2.

2.3.1 Computing R and T

As previously mentioned, we start with $\mathbf{S}$ and U as known variables. Since $\mathbf{S}$ and U are known (set as random values initially), their corresponding test functions, namely $\mathbf{S}^*$ and U^* as set to zeros. Thus the test functions introduced in equation (14) become:

$$\begin{cases} \mathbf{u}^* = \mathbf{R}^* \circ \mathbf{S} \\ p^* = T^* \cdot U \end{cases} \tag{15}$$

Computing the weak form of the governing equations (7) of the problem, leads to the following bilinear form c:

$$
\begin{aligned}
c\left(\mathbf{u}^*, \mathbf{u}\right) = \int_\Omega \left(\nabla^S \mathbf{u}^*\right) : \left(2\mu \nabla^S \mathbf{u}\right) d\Omega = \\
\frac{1}{2}\mu \int_\Omega \left(\nabla \mathbf{u}^* : \nabla \mathbf{u}\right) + \left(\nabla \mathbf{u}^* : \nabla \mathbf{u}^{\mathbf{T}}\right) + \left(\nabla \mathbf{u}^{*\mathbf{T}} : \nabla \mathbf{u}\right) + \left(\nabla \mathbf{u}^* : \nabla \mathbf{u}^{\mathbf{T}}\right) d\Omega = \\
\frac{1}{2}\mu \int_\Omega \left(\mathcal{R}^* \circ \mathcal{S}\right) : \left(\sum_{i=1}^{n-1} \mathcal{X}_i^{\mathbf{u}} \circ \mathcal{Y}_i^{\mathbf{u}} + \mathcal{R} \circ \mathcal{S}\right) + \\
\left(\mathcal{R}^* \circ \mathcal{S}\right) : \left(\sum_{i=1}^{n-1} \mathcal{X}_i^{\mathbf{u}} \circ \mathcal{Y}_i^{\mathbf{u}} + \mathcal{R} \circ \mathcal{S}\right)^T + \\
\left(\mathcal{R}^* \circ \mathcal{S}\right)^T : \left(\sum_{i=1}^{n-1} \mathcal{X}_i^{\mathbf{u}} \circ \mathcal{Y}_i^{\mathbf{u}} + \mathcal{R} \circ \mathcal{S}\right) + \\
\left(\mathcal{R}^* \circ \mathcal{S}\right)^T : \left(\sum_{i=1}^{n-1} \mathcal{X}_i^{\mathbf{u}} \circ \mathcal{Y}_i^{\mathbf{u}} + \mathcal{R} \circ \mathcal{S}\right)^T d\Omega
\end{aligned}
\tag{16}
$$

In a similar manner, we can replace the equations 15, 12 and 13 in the operators a and b. The equation solved at the current iteration is reduced to a $1D$ equation on x dimension only. This equation can be solved using any classical numerical technique, the finite elements for instance with P1/P1 interpollation functions on both the velocity and the pressure fields.

2.3.2 Computing S and U

Having computed $\mathbf{R}$ and T, we now use the obtained solutions to carry on with the fixed-point algorithm. The choice of the test functions becomes:

$$
\left\{
\begin{array}{l}
\mathbf{u}^* = \mathbf{R} \circ \mathbf{S}^* \\
p^* = T \cdot U^*
\end{array}
\right.
\tag{17}
$$

Replacing into the weak form of the problem leads to a one-dimensional partial differential equation, defined in the y dimension. Eventually the $1D$ problem is solved using classical numerical techniques, the finite elements for instance.

2.3.3 Continue the iterative process

After obtaining the $(\mathbf{S}, U)$ values, we repeat the steps detailed in section 2.3.1 then 2.3.2 until the convergence of the unknowns $(\mathbf{R}, \mathbf{S}, T, U)$. Once this convergence achieved, we can add another product of functions until the convergence of the residual of the differential equation of the problem.

3 Numerical example

The numerical method is applied to the benchmark problem of a lid-driven cavity flow. As shown in Fig.1 no slip conditions are enforced on all the cavity walls. The fluid on the top wall is moving horizontally at a velocity of $u_0 = 1m/s$. The computational domain is a square with a side length of $0.1m$, the working fluid has a density $\rho = 1kg/m^3$ and $\mu = 0.01Pa.s$, hence the flow Reynolds number in this example is $Re = 10$.

Writing the velocity field as $\mathbf{u} = (u_x, u_y)$ The results in Figs. 2, 3, 4 & 5 show respectively the distribution of the horizontal component of the velocity field u_x, the

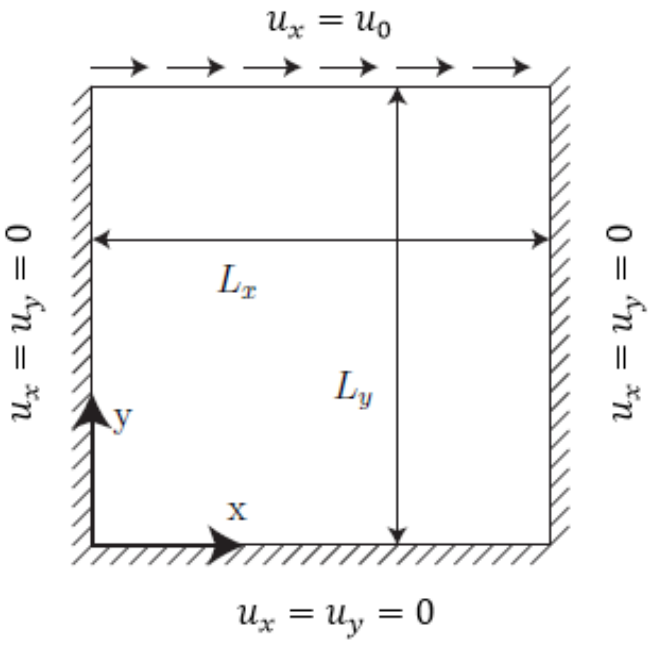

Figure 1: Geometry of the simulated lid-driven cavity flow

vertical component of the velocity filed u_y, the pressure field p and velocity vectors $\mathbf{u}$ at a chosen set of nodes.

4 CONCLUSIONS

In this work, we demonstrate the possibility of using the PGD along with the Galerkin Least Squares stabilization and a linearization fixed point iterative algorithm to find the solution of the Navier-Stokes equation in a fluid benchmark problem for low Reynolds numbers, using originally unstable P1/P1 formulations for the velocity and pressure fields. This work should be extended further for high Reynolds numbers with extra stabilization layers, using for example a multiscale method [20].

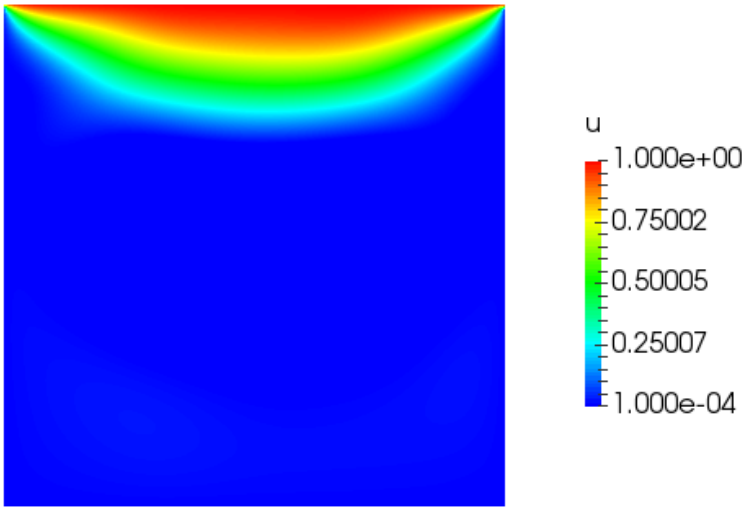

Figure 2: Horizontal velocity distribution in the simulated domain

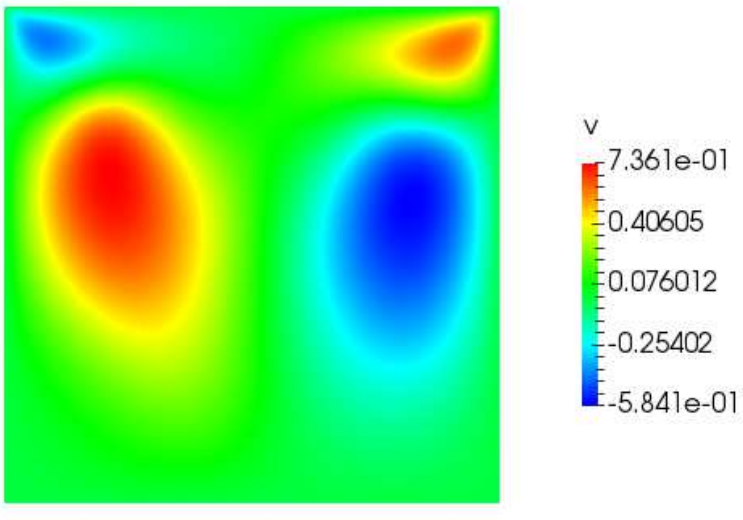

Figure 3: Vertical velocity distribution in the simulated domain

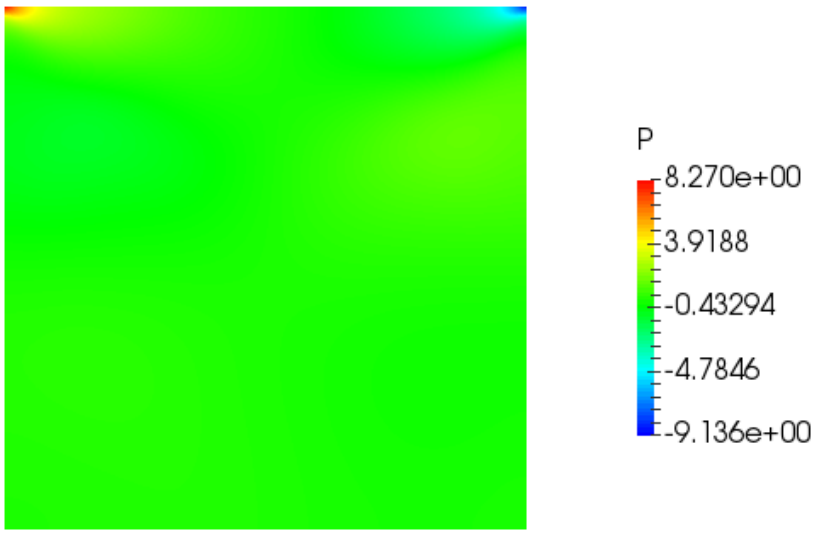

Figure 4: Pressure distribution in the simulated domain

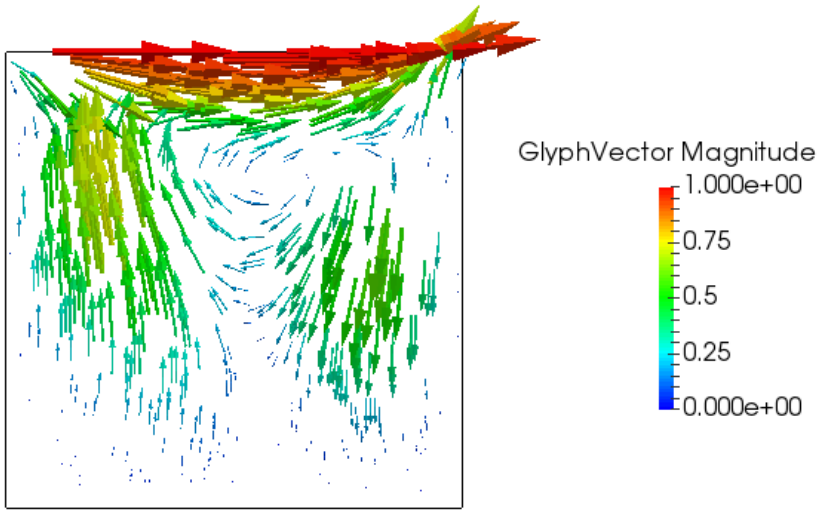

Figure 5: Velocity vectors showing the flow behavior in the simulated lid-driven cavity

REFERENCES

[1] Liu, X. and Li, L. Avariational multiscale stabilized finite element method for the Stokes flowproblem *Finite Elements in Analysis and Design*. (2006) **42**:580591.

[2] Chinesta, F., Keunings, R. and Leygue, E. *The proper generalized decomposition for advanced numerical simulations*. Springer, 2014.

[3] Chinesta, F., Leygue, A., Bognet, B., Ghnatios, C., Poulahon, F., Bordeu, F., Barasinski, A., Poitou, A., Chatel, S. and Maison-Le-Poec, S. First steps towards an advanced simulation of composites manufacturing by automated tape placement. *International journal of material forming*. (2014) **7**:8192.

[4] Aguado, J.-V., Borzacchiello, D., Ghnatios, C., Lebel, F., Upadhyay, R., Binetruy, C., Chinesta, F. A Simulation App based on reduced order modeling for manufacturing optimization of composite outlet guide vanes. *Advanced Modeling and Simulation in Engineering Sciences*. (2016) **4**:1-18.

[5] Bur, N., Joyot, P., Ghnatios, C., Villon, P., Cueto, E., Chinesta, F. On the use of model order reduction for simulating automated fibre placement processes. *Advanced Modeling and Simulation in Engineering Sciences*. (2016) **3**:1-18.

[6] Ghnatios, C., Abisset-Chavanne, E., Binetruy, C., Chinesta and Advani, S. 3d modeling of squeeze flow of multiaxial laminates. *Journal of Non Newtonian Fluid Mechanics*. (2016) **234**:188200.

[7] Ghnatios, C., Xu, G., Leygue, A., Visonneau, M., Chinesta, F. and Cimetiere, A., On the space separated representation when addressing the solution of PDE in complex domains. *Discrete & Continuous Dynamical Systems-S*. (2016) **9**:475-500.

[8] Ghnatios, C., Ammar, A., Cimetiere, A., Hamdouni, A., Leygue, A., Chinesta, F., First steps in the space separated representation of models defined in complex domains. *ASME 2012 11th Biennial Conference on Engineering Systems Design and Analysis*. (2012), ESDA 2012: 37-42.

[9] Aghighi, S., Ammar, A., Metivier, C., Normandin, M. and Chinesta, F. Non incremental transient solution of the rayleigh-benard convection model using the pgd. *Journal of Non Newtonian Fluid Mechanics*. (2013) **200**:6578.

[10] Dumon, A., Allery, C. and Ammar, A. Proper generalized decomposition (pgd) for the resolution of navier-stokes equations. *Journal of Computational Physics*. (2011) **230**:13871407.

[11] Ibanez, R., Abisset-Chavanne, E., Chinesta, F., and Huerta, A. Simulating squeeze flows in multiaxial laminates: Towards fully 3d mixed formulations. *International journal of material forming*. (2017) **10**:653669.

[12] Donea, J. and Heurta, A. *Finite element method for flow problem*, Wiley, 2003.

[13] Hughes, T., Feijoo, G., Mazzei, L. and Quincy, J. The variational multiscale method a paradigm for computational mechanics. *Computer methods in applied mechanics and engineering*. (1998) **166**:324.

[14] Hughes, T., Scovazzi, G., Bochev, P. and Buffa, A. A multiscale discontinuous galerkin method with the computational structure of a continuous galerkin method. *Computer methods in applied mechanics and engineering*. (2006) **195**:27612787.

[15] Bazilevs, Y., Calo, V., Cottrell, J., Reali, A. and Scovazzi, G. Variational multiscale residual-based turbulence modeling for large eddy simulation of incompressible flows. *Computer methods in applied mechanics and engineering*. (2007) **197**:173201.

[16] Coupez, T. and Hachem, E. Solution of high-reynolds incompressible flow with stabilized finite element and adaptive anisotropic meshing. *Computer methods in applied mechanics and engineering*. (2013) **267**:6585.

[17] Liu, X. and Li, S., A variational multiscale stabilized finite element method for the Stokes flow problem. *Finite Elements in Analysis and Design*. (2006) **42**:580591.

[18] Onate, J., Garcia, J., Idelsohn, S. Computation of the stabilization parameter for the finite element solution of the advective-diffusive problems. *International Journal of numerical methods fluid*. (1997) **25**:13851407.

[19] C. Ghnatios, Simulation avancée des problemes thermiques rencontrés lors de la mise en forme des composites. PhD thesis, Ecole Centrale de Nantes, Octobre 2012.

[20] Hachem, E., Rivaux, B., Kloczko, T., Digonnet, H. and Coupez, T. Stabilized finite element method for incompressible flows with high Reynolds number. *Journal of Computational Physics*. (2010), **229**:86438665.